# Demonstration of a Sagnac-Type Cold Atom Interferometer with Stimulated Raman Transitions *

WANG Ping(王平)[1,2,3], LI Run-Bing(李润兵)[1,2,3], YAN Hui(颜辉)[1,2,3], WANG Jin(王谨)[1,2], ZHAN Ming-Sheng(詹明生)[1,2**]

[1]State Key Laboratory of Magnetic Resonance and Atomic and Molecular Physics, Wuhan Institute of Physics and Mathematics, Chinese Academy of Sciences, Wuhan 430071

[2]Center for Cold Atom Physics, Chinese Academy of Sciences, Wuhan 430071

[3]Graduate School, Chinese Academy of Sciences, Beijing 100080

(Received 9 October 2006)

*Cold-matter-wave Sagnac interferometers possess many advantages over their thermal atomic beam counterparts when they are used as precise inertial sensors. We report a realization of a Sagnac-type interferometer with cold atoms. Cold rubidium atoms are prepared in a magneto-optical trap and are pushed by resonant laser pulse to form slow atomic beam. In the interference region, atomic wave packets are coherently manipulated using $\pi/2-\pi-\pi/2$ Raman pulse sequences. Interference fringes with maximum contrast of 37% are observed experimentally.*

*PACS: 03. 75. Dg, 39. 20. +q, 42. 50. Vk, 06. 30. Gv*

Atom interferometry[1−4] works with matter wave, and meanwhile acts as the test bed of the wave character of matter. Because atoms have rest mass contrary to photons and can interact with other matter much easier than neutron, interferometers using atoms have proven their importance in testing the foundations of quantum mechanics, manipulating the wave functions coherently and in metrology of time and frequency, and other applications as precise inertial sensors such as gyroscopes and accelerometers.

Early atom interferometers have used thermal atomic beams.[5,6] Since the invention of laser cooling and trapping techniques was reported, laser cooled atoms have been widely used in the atom interferometry experiments. Examples of cold atom interferometers include exact measurement of the Newtonian constant of gravitation $G$ and absolute-gravity-gradient,[7−10] accurate measurement of photon recoil,[11] and precise determination of the fine-structure constant $\alpha$.[12] More recently, even ultracold Bose–Einstein condensed atoms have also been used by Torii *et al.* in constructing a Mach–Zehnder interferometer and in studying the optical Bragg diffraction.[13] The experimental setup for a cold atom interferometer is usually in vertical configuration similar to the atom fountain, in which the atomic wave packets interfere along the gravity direction. This quite fits the need of measuring gravity and general interferometry experiments. However, this type of configuration is not convenient for rotation measurement.

Sensitivity to rotation due to Sagnac effect can be enhanced greatly by using atoms instead of photons. The phase shift of a Sagnac interferometer is expressed by

$$\Delta\phi = \frac{4\pi\Omega A}{\lambda_d V},$$

where $\Omega$ is the angular velocity of rotation, $A$ is the area enclosed by interference loop, and $V$ is the particle velocity. The de Broglie wavelength of moving particle is $\lambda_d = h/mV$ with $m$ being the particle mass. Since the atom mass $m$ is much larger than the photon mass $hv/c^2$, the sensitivity of atom interferometer is increased by a factor of about $10^{10}$ over a light interferometer.

To sense a rotation, atom interferometers are configured as the Sagnac-type interferometers in which an enclosed area is formed by two indistinguishable paths. In this case, taking the gravity into account, horizontal configuration was usually used. For example, Lenef *et al.*[5] measured the phase shift induced by rotation of an atom interferometer, Gustavson *et al.*[6] realized the most accurate atom gyroscope using thermal atomic beam. In practice, to achieve high sensitivity high flux of atoms is required. To reduce the dimension of the gyroscope, low atomic velocity is preferred. Thus a Sagnac-type atom interferometer with laser cooled atoms has been expected for a long time. However, the prototype inertial sensor using cold-atom interferometry was realized only recently.[14]

Here we introduce a new compact transverse cold atom interferometer based on the magneto-optical trap (MOT) and low velocity cold atom beam techniques. Cold atoms were firstly prepared in MOT, and then pushed by a resonance laser pulse to the interference area. A $\pi/2-\pi-\pi/2$ Raman pulse sequence

* Supported by the National Basic Research Program of China under Grant No 2005CB724505/1.

** To whom correspondence should be addressed. Email: robinwp@wipm.ac.c

was used to coherently manipulate atomic wave packets. The velocity of cold atom cloud can be precisely controlled by adjusting the intensity or duration of pushing pulse. The distance between two Raman interaction areas can be greatly reduced by using low velocity atoms. In our experiment, this distance is only 12 cm as compared with 100 cm that was used in thermal atom experiments.[5,6] Clear interference fringe was successfully observed with contrast of 37%.

The theory of atom interferometer is based on a three-level system underlying the two-photon stimulated Raman transition.[15] As shown in Fig. 1, laser fields ($\omega_1$ and $\omega_2$) can couple states $|g\rangle$ and $|e\rangle$ by an intermediate state $|i\rangle$. The atom first absorbs one photon with frequency $\omega_1$, and then is stimulated to emit one photon with frequency $\omega_2$. The large detuning $\Delta$ of the laser frequencies from the excited state $|i\rangle$ greatly inhibits the spontaneous decay, and the system can be treated as a two-level system.

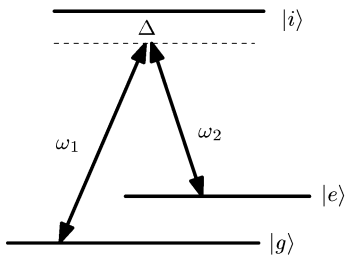


**Fig. 1.** Diagram of a three-level atom driven by two laser fields.

The Hamiltonian for the three-level system reads

$$H = \hbar\omega_g|g\rangle\langle g| + \hbar\omega_i|i\rangle\langle i| + \hbar\omega_e|e\rangle\langle e| - \boldsymbol{d}\cdot\boldsymbol{E}. \tag{1}$$

The field in which atoms suffered can be described as a superposition of two individual laser fields,

$$\boldsymbol{E} = \boldsymbol{E}_1\cos(\boldsymbol{k}_1\cdot\boldsymbol{x} - \omega_1 t + \phi_1) + \boldsymbol{E}_2\cos(\boldsymbol{k}_2\cdot\boldsymbol{x} - \omega_2 t + \phi_2). \tag{2}$$

The effective Rabi frequency $\Omega_{\rm eff}$ of coupling the two ground states is expressed as

$$\Omega_{\rm eff} = \frac{\Omega_1\Omega_2}{2\Delta}, \tag{3}$$

where $\Omega_1$ and $\Omega_2$ are the single-photon Rabi frequencies, respectively. Suppose that the atom is initially prepared in the superposed state of the two ground states, i.e.

$$|\Psi(t_0)\rangle = C_e(t_0)|e\rangle + C_g(t_0)|g\rangle. \tag{4}$$

After interacting with the Raman lasers for a certain time $\tau$, the atom has the following new probability amplitude in the $|g\rangle$ state by solving the Schrödinger equations[2]

$$\begin{aligned} C_g(t_0+\tau) &= C_g(t_0)\cos\left(\frac{\Omega_{\rm eff}\tau}{2}\right) - iC_e(t_0)e^{i\varphi(t_0)}\sin\left(\frac{\Omega_{\rm eff}\tau}{2}\right), \\ C_e(t_0+\tau) &= C_e(t_0)\cos\left(\frac{\Omega_{\rm eff}\tau}{2}\right) - iC_g(t_0)e^{-i\varphi(t_0)}\sin\left(\frac{\Omega_{\rm eff}\tau}{2}\right), \end{aligned} \tag{5}$$

where $\varphi(t_0)$ is defined as

$$\varphi(t_0) = \omega_0 t_0 - \boldsymbol{k}_{\rm eff}\cdot\boldsymbol{z} + \varphi_i^0, \tag{6}$$

and $\varphi_i^0$ represents the effective initial phase of the Raman lasers; $\boldsymbol{k}_{\rm eff}$ denotes effective Raman propagation vector. We can see from Eq. (5) that by interacting with the Raman lasers, the atom evolves into a new state in which the phase of laser is imprinted. These processes are described by

$$|e\rangle \to e^{-i\varphi(t_0)}|g\rangle, \tag{7}$$

$$|g\rangle \to e^{i\varphi(t_0)}|e\rangle. \tag{8}$$

The external degrees of freedom of the atom are also changed along with this internal state transition. In the Sagnac-type interferometer, $k$-vector of the Raman lasers is perpendicular to atomic motion, and the two laser beams are chosen in co-propagating (Doppler insensitive) or counter-propagating (Doppler sensitive) configurations. In co-propagating configuration, atom acquires recoil kick of the photons about $\hbar(\boldsymbol{k}_1 - \boldsymbol{k}_2) = \hbar(|\boldsymbol{k}_1| - |\boldsymbol{k}_2|)$, which is quite smaller as compared with $\hbar(\boldsymbol{k}_1 - \boldsymbol{k}_2) = \hbar(|\boldsymbol{k}_1| + |k_2|)$ in the counter-propagating case.

The Raman pulse sequence $\pi/2-\pi-\pi/2$ will shape an interference loop to sense the rotation. The first $\pi/2$ pulse separates the atom into two paths, and puts atom into a superposition internal state simultaneously. The following $\pi$ pulse reflects the atom, and the internal states are swapped. The last $\pi/2$ pulse recombines the atom wave packet. The relative phases $\varphi(t_1)$, $\varphi(t_2)$ and $\varphi(t_3)$ of the three pairs of Raman pulses are related to the population in the following way:

$$\begin{aligned} P_{e,g} &= \frac{1}{2}[1 \pm \cos(\varphi(t_1) - 2\varphi(t_2) + \varphi(t_3))] \\ &= \frac{1}{2}[1 \pm \cos(\Delta\Phi)]. \end{aligned} \tag{9}$$

If one changes $\varphi(t_3)$ while keeping $\varphi(t_1)$ and $\varphi(t_2)$ unchanged, the state population will be changed with $\varphi(t_3)$ in the form of a cosine function.

Figure 2 shows our experimental setup. An aperture of 3 mm diameter is placed between the two chambers to preserve the pressure difference. The interference region is 23 cm long, and at the end of the

chamber a photo multiplier tube (PMT) is used to detect the fluorescence induced by a resonant probe leaser. Three pairs of counter-propagating trapping beams are (1, 1, 1) configuration. Each pairs is $\sigma^+ - \sigma^-$ polarized with equal intensity. The water-cooled magnetic coils can generate magnetic field with gradient of 20 Gauss/cm at the MOT centre. The laser frequency is locked to $^{85}$Rb transition[16,17] by saturation absorption spectroscopy techniques, and the line width of laser frequency is less than 1 MHz. The frequency and intensity of trapping beam are controlled by using an acousto-optical modulator (AOM) in a double-pass configuration. The trapping beam was split into six equal-intensity beams by combining half-wave plates (HWPs) and polarization-beam-splitters (PBSs). A single-mode polarization-maintenance optical fibre is used to transmit and to spatially filter all the laser beams from the optical desk to the vacuum chambers. Three pairs of Helmholtz coils are used to compensate for or cancel the Earth magnetic fields. The whole experimental apparatus is mounted on a vibration isolation optical table (Newport RS-4000 floating on I-2000 legs) to reduce the random vibration.

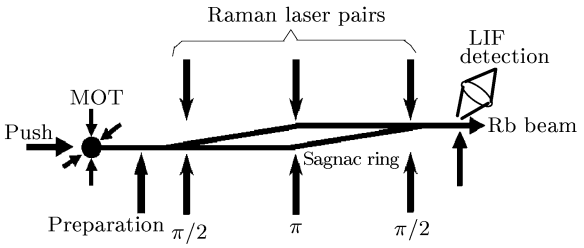


**Fig. 2.** Experimental arrangement of the transverse cold atom Sagnac-type interferometer. Cold Rb atoms are prepared in the magneto-optical trap (MOT). Push laser pulse loads the atom cloud to the interference region consisting of Raman laser pulse sequence $\pi/2-\pi-\pi/2$. Laser-induced fluorescence (LIF) signal is recorded in the probe region.

Two-photon Raman[18,19] pulse drives Rabi oscillations between two hyperfine levels of the ground state. When a correct Raman pulse-pair sequence is chosen, and the propagation axis of each Raman pulse-pair beams co-propagate or counter-propagate, the interference phenomenon of atoms will be displayed. As illustrated in Fig. 2, three Raman laser pairs work in a continuous way. The pulse area defined as $\pi/2$ or $\pi$ is determined by changing the laser intensity for the given transit time of moving atom through the Raman beam. A Raman laser pair is generated by the $\pm 1$ order output[20,21] from an AOM (Brimrose GPF-1500-200-.780) with carry frequency of 1.5 GHz supplied by an analogue signal generator (HP/Agilent E8257C PSG), which is externally referenced to a hydrogen atomic clock (Shanghai Astronomical Observatory SOHM-Ⅲ). The main laser (TOPTICA TA100) is locked to the crossover peak of $F = 3 \rightarrow F' = 2$ and $F = 3 \rightarrow F' = 4$ (see Fig. 3). The Raman lasers R1 and R2 are phase-correlated with each other, and they also have a stable frequency difference of 3.0 GHz, which is exactly equal to the energy level separation of two ground states of $^{85}$Rb. Meanwhile R1 and R2 are commonly detuned about 1.5 GHz from the $5P_{3/2}$, $F' = 3$ hyperfine level.

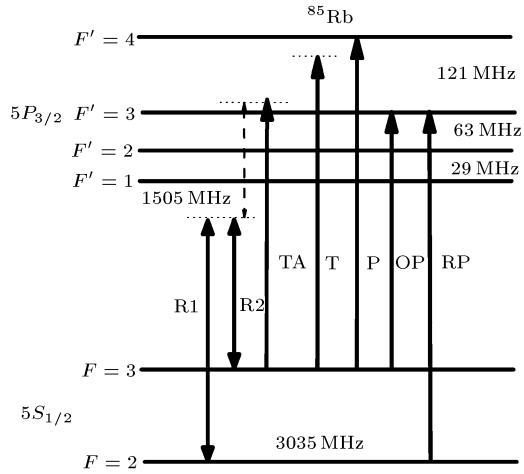


**Fig. 3.** $^{85}$Rb atomic energy levels and laser frequencies. The frequency of main laser (TA) is locked to the $F = 3 \rightarrow F' = (2, 4$ crossover) resonance peak. Raman transition is realized between the ground states of $5^2\ S_{1/2}$ ($F = 2$) and $5^2\ S_{1/2}$ ($F = 3$) by two Raman beams R1 and R2. T: trapping laser, P: probe laser, OP: optical pumping laser, RP: repumping laser.

The two Raman beams are overlapped with orthogonal linear polarizations by a PBS cube and then are coupled into the fibre. Because any change in the relative paths of the two Raman beams due to vibrations of the beam steering optics will be seen as spurious interference phase shift, vibration isolation is necessary. Co-propagating beams in the optic fibre also minimize the potential phase shift of the Raman light. The fibre filtered Gaussian beam is collimated, its diameter ($1/e^2$ intensity contour) is about 1 cm, and it is divided into three parts as $\pi/2 - \pi - \pi/2$ pulse pairs. An electro-optical modulator (EOM, New Focus 4002) is used as a phase modulator to change the relative phase of the final $\pi/2$ pulse, $\varphi(t_3)$. The intensity ratio of Raman beam-pair R1:R2 can be optimized to minimize unwanted ac Stark shifts.[18]

Atoms are firstly cooled and about $10^8$ atoms are trapped in the MOT[22] within 1 s, the cold atom cloud is pushed transversely by a 700 $\mu$s duration resonant light pulse[23] to the interference chamber at a speed of 24 m/s. The cold atomic flux will spend around 30 ms to fly across the Raman laser pairs and to the detection region. An optical pumping (OP) light (shown in Fig. 3, or preparation light in Fig. 2) resonant with the $5S_{1/2}$, $F = 3 \leftrightarrow 5P_{3/2}$, $F' = 3$ tran-

sition is applied to pump all atoms to $F = 2$. Magnetic insensitive Zeeman sublevel, $m_F = 0$, is chosen for investigation of atomic interference. Other Zeeman sublevels are shifted out of resonance of Raman laser pair. Following state preparation, atoms interact with the $\pi/2 - \pi - \pi/2$ Raman pulse sequence. A vertical bias field, produced by a rectangle Helmholtz coil pair, is applied to define a quantization axis. When atoms are driven by the first $\pi/2$ Doppler insensitive Raman pulse, they will coherently evolve into superposition of two ground states, $F = 2$, $m_F = 0$ and $F = 3$, $m_F = 0$. After 4.8 ms free flight, atoms travel through the $\pi$ pulse and exchange their states. Then the atoms travel through the second $\pi/2$ pulse, and the wave packets interfere with each other. The fluoresce induced by the probe laser from the state $F = 3$, $m_F = 0$ is recorded to analyse the state population.

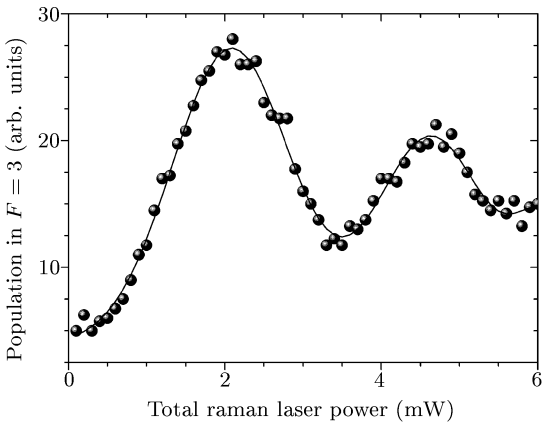


**Fig. 4.** Rabi oscillations for co-propagating Raman beams with detuning $\Delta = 1.5$ GHz. The circles shows the experimental relative population of state $F = 3$ versus total Raman laser intensity (the ratio of the two lasers R1/R2 is 1:5.3). The solid curve shows the fitting.

We have observed Rabi oscillations when varying total Raman-pair intensity while keeping the intensity ratio constant (1:5.3). Raman beams are in co-propagating configuration, and the frequencies are detuned with $\Delta = 1.5$ GHz away from the resonances. The experimental result is shown by the circles in Fig. 4, and the fitting result is illustrated by the solid line. The circles show clearly the dependence of population of the $F = 3$ state on intensity of Raman beams, it is a gradually attenuation sine wave, and the maxima appear at 2.1 mW/cm$^2$ and 4.7 mW/cm$^2$.

At this stage, we can define the pulse width ($\pi$ or $\pi/2$) experimentally. We then change the optical phase of the final $\pi/2$ pulse gradually by adjusting the voltage applied to the EOM while recording the fluoresce intensity which is proportional to population of the $F = 3$ state. A typical interference fringe is shown in Fig. 5, the circles show the experimental data, and the solid line is the fitting to Eq. (9). The half-wave voltage of the EOM is 125 V. There are two complete oscillation cycles from 0 to 500 V. The relative maximum population is 11, and the minimum population is 5, which gives the fringe contrast of 37%.

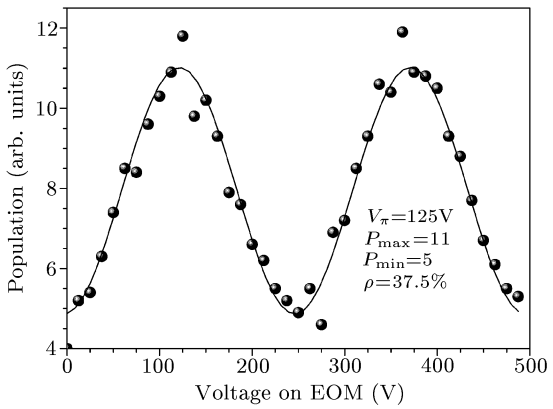


**Fig. 5.** Interference fringe as a function of relative population to the voltage applied to the EOM. The half-wave voltage of the EOM is 125 V.

In conclusion, we have developed a compact transverse cold $^{85}$Rb atom interferometer. A 1.5 GHz AOM is adopted to produce a pair of Raman lasers, and an EOM is used to change the optical phase of a $\pi/2$ pulse. We have successfully realized the cold atom preparation, pushing, optical pumping, Raman population transfer, and finally observed high contrast interference fringe. Following this development of the cold atom Sagnac-type interferometer, the measurement of rotation (atom gyroscope) is underway.

# References

[1] Adams C S et al 1994 *Adv. At. Mol. Opt. Phys.* **34** 1
[2] Berman P R (ed.) 1997 *Atom Interferometry* (San Diego: Academic) and references therein
[3] Arlt J et al 2005 *Adv. At. Mol. Opt. Phys.* **50** 55
[4] Zhou S K and Zhan M S 1993 *Chinese J. Quantum Electron.* **10** 91 (in Chinese)
[5] Lenef A et al 1997 *Phys. Rev. Lett.* **78** 760
[6] Gustavson T L et al 1997 *Phys. Rev. Lett.* **78** 2046
[7] McGuirk J M et al 2002 *Phys. Rev.* A **65** 033608
[8] Peters A et al 2001 *Metrologia* **38** 25
[9] Snadden M J et al 1998 *Phys. Rev. Lett.* **81** 971
[10] Peters A et al 1999 *Nature* **400** 849
[11] Weiss D S et al 1993 *Phys. Rev. Lett.* **70** 2706
[12] Wicht A et al 2002 *Physica Scripta* **T102** 82
[13] Torii Y et al 2000 *Phys. Rev.* A **61** 041602
[14] Canuel B et al 2006 *Phys. Rev. Lett.* **97** 010402
[15] Kasevich M and Chu S 1992 *Appl. Phys. B: Photophys. Laser Chem.* **54** 321
[16] Jiang K J et al 2003 *Chin. Opt. Lett.* **1** 377
[17] Wang J et al 2000 *Chin. J. Quantum Electron.* **17** 43 (in Chinese)
[18] Kasevich M et al 1991 *Phys. Rev. Lett.* **66** 2297
[19] Moler K et al 1992 *Phys. Rev.* A **45** 342
[20] McGuirk J M et al 2000 *Phys. Rev. Lett.* **85** 4498
[21] Bouyer P et al 1996 *Opt. Lett.* **21** 1502
[22] Wang J et al 2000 *Acta Opt. Sin.* **20** 862 (in Chinese)
[23] Jiang K J et al 2005 *Chin. Phys. Lett.* **22** 324